Article

Rational Design of Bioelectrochemically Multifunctional Film with Oxidase, Ferrocene, and Graphene Oxide for Development of In Vivo Electrochemical Biosensors

Xiuyun Wang, Qian Li, Jingjing Xu, Shuo Wu, Tongfang Xiao, Jie Hao, Ping Yu, and Lanqun Mao

Anal. Chem., **Just Accepted Manuscript** • DOI: 10.1021/acs.analchem.6b00720 • Publication Date (Web): 05 May 2016

Rational Design of Bioelectrochemically Multifunctional Film with Oxidase, Ferrocene, and Graphene Oxide for Development of In Vivo Electrochemical Biosensors

Xiuyun Wang,[†] Qian Li,[†] Jingjing Xu,[†] Shuo Wu,[†] Tongfang Xiao,[‡] Jie Hao,[‡] Ping Yu,[‡] Lanqun Mao[*,‡]

[†] *School of Chemistry, Faculty of Chemical, Environmental and Biological Science and Technology, Dalian University of Technology, Dalian 116024, China*

[‡] *Beijing National Laboratory for Molecular Sciences, Key Laboratory of Analytical Chemistry for Living Biosystems, Institute of Chemistry, the Chinese Academy of Sciences (CAS), Beijing 100190, China*

[*] Corresponding Author: Tel: +86-10-62646525; E-mail: lqmao@iccas.ac.cn.

ABSTRACT

This study demonstrates a new strategy to develop in vivo electrochemical biosensors through rational design and simple formation of bioelectrochemically multifunctional film (BMF). The BMF is rationally designed by first efficiently incorporating oxidase, ferrocene mediator, and graphene oxide into polymaleimidostyrene/polystyrene (PMS/PS) matrix to form a homogenous mixture and then simply formed by drop-coating the mixture onto solid conducting substrate. By using the as-formed BMF, electrochemical biosensors could be constructed with a technical simplicity and high reproducibility. To illustrate the BMF-based biosensors for in vivo applications, we directly couple the biosensors to in vivo microdialysis to establish an online electrochemical system (OECS) for in vivo monitoring of glucose in rat auditory cortex during salicylate-induced tinnitus model. The OECS with the BMF-based biosensor as the detector shows a linear response toward glucose within a concentration range from 50 to 500 μM with a detection limit of 10 μM (S/N = 3). Additionally, the OECS is stable and does not suffer from the interference from the electroactive species endogenously coexisting in the brain microdialysate. With the BMF-based OECS, the basal level of glucose in the microdialysate continuously sampled from rat auditory cortex is determined to be 120 ± 10 μM (n = 5). After the rats were administrated with salicylate to induce transient tinnitus, the microdialysate glucose concentration in the rat auditory cortex remarkably increased to 433 ± 190 μM (n = 5) at the time point of 1.5 h. This study essentially offers a new, technically simple and reproducible approach to development of in vivo electrochemical biosensors, which is envisaged to be relatively useful for understanding of the molecular basis of brain functions.

INTRODUCTION

One of the main focuses underlying research community of brain chemistry lies in revealing and understanding of chemical processes behind in physiological and pathological events and such focus has been of a particularly great concern over recent a few years.[1-8] Quantitative monitoring of neurochemicals in the extracellular brain environment would pave a straightforward avenue to the researches into brain chemistry and is, therefore, of great importance in understanding the molecular basis of brain functions.[9-14] Among the methods employed for in vivo neurochemical measurements, electrochemical methods with enzyme-based biosensors are particularly useful because the use of enzymes as the biorecognition elements for the biosensing of neurochemicals substantially endows the electrochemical biosensors with excellent properties including high selectivity and sensitivity, and applicability to a large number of target neurochemicals.[14-20] However, the construction of biosensors normally involves several step-by-step procedures for surface confinement of enzyme recognition elements (e.g., oxidases, dehydrogenases) and electronic transducers (e.g., electron transfer mediators for oxidases, and cofactors and electrocatalysts for dehydrogenases), which renders a technically complicated and time-consuming process for biosensor construction, and inevitably confronts the problems in the reproducibility for biosensor construction.[21-26] These limitations essentially keep the enzyme-based biosensors far from the physiological and pathological investigations although they have been demonstrated to be potentially useful for the applications in various research fields.[27]

To overcome the limitations mentioned above, we have recently developed some strategies to simplify the procedures for the construction of the biosensors and thereby minimize the biosensor-to-biosensor deviation. For instance, by successfully synthesizing ionic liquids with enzyme cofactor (i.e., reduced form of nicotinamide adenine dinucleotide, NAD) as the anion, we have been able to prepare a multifunctional gel consisting of

methylene green electrocatalyst and carbon nanotubes. The gel could be easily and reproducibly mounted onto electrode surface and is used for transducing the biorecognition events to signal readout with a high efficiency.[28-30] The other strategy we have developed is basically based on rational inclusion and adaptive encapsulation of all biosensing elements into an infinite coordination polymer nanoparticle and the biosensors could be reproducibly produced simply by confining the bioelectrochemically active nanoparticles on electrode surface.[31-32] The combination of the excellent analytical properties inherent in the enzyme-based biosensors with the good reproducibility of the biosensor construction essentially enabled us to use electrochemical biosensors to monitor the dynamic change of neurochemicals in the central nervous system.[33-34]

Inspired by our earlier attempts described above, we demonstrate here a new strategy to reproducibly prepare in vivo electrochemical biosensors by rational designing and one-step formation of bioelectrochemically multifunctional film (BMF). The BMF is rationally designed by efficiently incorporating oxidase, ferrocene (Fc) electron transfer mediator, graphene oxide (GO) into polymaleimidostyrene (PMS) and polystyrene (PS) matrix to form a homogenous dispersion and then simply formed by drop-coating the dispersion onto electrode substrate (Scheme 1 A). The BMF-based biosensors are well responsive to the target (i.e., glucose that is used as an example in this study) with a good stability. To study the validity of the simply-formed BMF-based biosensors for in vivo monitoring of physiologically important species (i.e., glucose in this study) in the central nervous system, the biosensors are directly coupled to in vivo microdialysis to form an online electrochemical system (OECS, Scheme 1 B) to monitor the dynamic change of glucose in the microdialysate continuously sampled from the auditory cortex of rat brain during salicylate-induced tinnitus model with a high reliability and robustness. The strategy demonstrated here for the development of in vivo electrochemical biosensors is relatively

versatile for other kinds of neurochemicals, for example, by replacing glucose oxidase used here with other kinds of oxidases. This is study essentially opens a new approach to in vivo electrochemical biosensing, which is envisaged to be of great importance in understanding the molecular basis underlying brain functions.

EXPERIMENTAL SECTION

Chemicals and Solutions. Epinephrine (E), norepinephrine (NE), uric acid (UA), ascorbic acid (AA), 3, 4-dihydroxyphenylacetic (DOPAC), dopamine (DA), glucose oxidase (GOD, EC 1.1.3.4, from *Aspergillus Niger*, 158 U mg^{-1}), ascorbate oxidase (EC 1.10.3.3, from *Cucurbita species)*, glucose, Fc, and PS (Mw ~1110) were all purchased from Sigma and used as supplied. PMS (M_n = 3600, M_w/M_n = 1.12) was supplied by Saitama Institute of Technology, Japan and could be synthesized with the procedures reported previously.[35] Artificial cerebrospinal fluid (aCSF) used both as the electrolyte for electrochemical experiments and as the perfusion solution for in vivo microdialysis was prepared by mixing NaCl (126 mM), KCl (2.4 mM), KH_2PO_4 (0.5 mM), $MgCl_2$ (0.85 mM), $NaHCO_3$ (27.5 mM), Na_2SO_4 (0.5 mM), and $CaCl_2$ (1.1 mM) into Milli-Q water. PMS, PS and Fc were dissolved in chloroform. All aqueous solutions were prepared with Milli-Q water.

An aqueous dispersion of GO was prepared according to previous reports.[36] Briefly, graphite oxide synthesized from graphite by a modified Hummers method [37] was first dispersed into water, and the dispersion was then subject to dialysis to remove residual salts and acids. The resulting suspension was again dispersed into water to form a dispersion of GO (0.05 wt %). The resulting dispersion was subject to 30 min of centrifugation at 3000 rpm to remove any unexfoliated graphite oxide. After that, 10.0 mL of the aqueous dispersion of exfoliated GO (0.5 mg mL^{-1}) was mixed with 10.0 mL of aqueous solution, in which 10.0 μL of an aqueous solution of hydrazine (35 wt %) and 70.0 μL of an aqueous

solution of ammonia (28 wt %) were added. The resulting mixture was then vigorously stirred for 5 min and finally put in a water bath (95 °C) for 1 h to produce a stable aqueous dispersion of GO.

Apparatus and Measurements. All electrochemical experiments were performed with a computer-controlled CHI 1030 electrochemical workstation (CHI Instruments, Shanghai, China) at room temperature using aCSF as supporting electrolyte. In OECS, a thin-layer radial electrochemical flow cell was used as the detector. The cell consists of a thin layer radial flow block with a 50 μm of gasket, a single GC electrode (6 mm in diameter) as working electrode, stainless steel as counter electrode, and an Ag/AgCl (KCl-saturated) electrode as reference electrode. GC electrodes used in both off-line and online electrochemical measurements were polished first with emery paper (2000 mesh) and then with aqueous slurries of fine alumina powder (0.3 and 0.05 μm) on a polishing cloth. The electrodes were finally rinsed with ethanol and Milli-Q water under an ultrasonic bath, each for 5 min. In vitro electrochemical measurements were conducted in a conventional electrochemical cell with a three-electrode configuration with GC electrode (3 mm in diameter) as working electrode, a platinum spiral wire as counter electrode and an Ag/AgCl electrode (KCl-saturated) as reference electrode. Scanning electron microscopy (SEM) image was performed on scanning electron microscopy (FEI Quanta 450, FEI Company, USA)

BMF Formation and Biosensor Preparation. To prepare BMF, 10 μL of aqueous solution of GOD (1.8 kU mL^{-1}), 10 μL of aqueous dispersion of GO (5 mg mL^{-1}), 5 μL of PMS in chloroform (5 mg mL^{-1}), 5 μL of PS in chloroform (10 mg mL^{-1}), and 10 μL of Fc in chloroform (10 mg mL^{-1}) were mixed to form a homogeneous dispersion under vigorous stirring. After that, 8 μL of the as-formed dispersion was drop-coated onto GC electrode and the electrode was dried in air to form BMF onto electrode surface. The BMF-coated GC

electrodes were thus used as the electrochemical biosensor for glucose measurements. To further validate the BMF-based biosensors for selective in vivo measurements, 2 μL of ascorbate oxidase (10 mg mL^{-1}) was over-coated onto the surface of the electrodes to eliminate the interference from ascorbic acid in the extracellular fluid of rat brain.

In Vivo Microdialysis and Online Electrochemical Measurements. Surgery for in vivo microdialysis was performed as reported previously.[38-39] Briefly, adult rats (350-400g) purchased from Experimental Animal Center of Peking University were served as subjects. The rats were housed on a light-dark schedule (12:12 h) with food and water *ad libitum*. After being anaesthetized with chloral hydrate (345 mg kg^{-1}, i.p.), the rats were positioned onto a stereotaxic frame. The microdialysis guide cannulas were carefully implanted in the auditory cortex (AP = -4.0 mm, L = 6.5 mm from bregma, V = 2.0 mm from the surface of the skull) according to standard stereotaxic procedures.[40] The guide cannula was fixed with three skull screws and dental cement. A stainless steel dummy blocker was inserted into the guide cannula and fixed until the insertion of the microdialysis probe (CMA, dialysis length, 4 mm; diameter, 0.24 mm). The body temperature of the rats was maintained at 37 °C with a heating pad during the surgeries and an anesthetic was supplemented if necessary. Immediately after the surgery, the rats were placed into a warm incubator individually until they recovered from the anesthesia and were allowed to recover for at least 24 h prior to the surgeries for in vivo microdialysis sampling.

For in vivo glucose measurements in the central nervous system, the BMF-based biosensor was positioned into the thin-layer electrochemical flow cell and used as the detector to selectively monitor glucose in the microdialysates continuously sampled from the rat auditory cortex (Scheme 1 B). Prior to the online measurements, the microdialysis probe was implanted in rat auditory cortex and allowed to equilibrate for at least 90 min by continuously perfusing the probe with aCSF. The microdialysates were continuously

sampled with microinjection pump (CMA 100, CMA Microdialysis AB, Stockholm, Sweden) with aCSF as the perfusion solution at a flow rate of 2 μL min^{-1}. Prior to the investigation on the dynamic change of microdialysate glucose level following salicylate-induced tinnitus, we further studied the applicability of the BMF-based OECS for in vivo monitoring glucose by continuously measuring microdialysate glucose level with intraperitoneal (*i.p.*) injection of insulin (5 U). To study the change of the glucose level in the microdialysate collected from rat auditory cortex following tinnitus, sodium salicylate (121 mg mL^{-1}) was dissolved into 0.1 M phosphate buffer (pH 7.4) and injected to the animals (345 mg kg^{-1}, *i.p.*). Such a dose of sodium salicylate was reported to be able to produce an animal model oftinnitus.[41-42] Before and after the injection of sodium salicylate, the microdialysate glucose was continuously monitored with the BMF-based OECS (Scheme 1 B).

RESULTS AND DISCUSSION

Design and Formation of BMF. In this study, we chose PMS/PS as a matrix to form the bioelectrochemically multifunctional film because, in the previous studies,[43-44] PMS/PS matrix has been demonstrated to provide a biologically compatible microenvironment to maintain the activity of enzymes and could thus be particularly useful for the development of enzyme-based biosensors. This property was actually benefited from the film-forming ability of PS and the conjunctive role of PMS; in the PMS/PS matrix, maleimide moieties of PMS react with sulphydryl or amino groups of oxidase enzymes, enabling oxidase enzymes to be covalently attached to PMS with a high stability and to retain their biological activity in PS film.[43-44] Unlike the biosensors developed in those previous studies with the PMS/PS as a matrix, which were normally based on the determination of the consumption of oxygen or the generation of hydrogen peroxide involved in the enzymatic reactions (i.e., first-generation biosensors), we wish to develop redox-mediated second-generation

electrochemical biosensors with the PMS/PS matrix in this study because this kind of biosensors are more suitable for in vivo monitoring of neurochemicals in the central nervous system due to their lower dependence of oxygen variation and less production of biologically toxic hydrogen peroxide during the biosensing process.[30] For this purpose, GOD that was used as an example enzyme in this study was dissolved into the mixture containing PMS and PS. To shuttle the electron transfer between GOD and electrode, an electron transfer mediator with efficient electron transfer rate in the matrix remain very essential. Moreover, to achieve excellent analytical properties for the BMF-based biosensors, the BMF should have a good electrical conductivity, high stability, and simplicity-in-operation.

Based on the consideration mentioned above, the BMF is rationally designed to simultaneously and efficiently incorporate oxidase (i.e., GOD), electron transfer mediator and conducting materials in the PMS/PS matrix. To make an electrically conducting BMF, GO was included in the matrix in this study in terms of its good conductivity and nanosheet structure as well as good dispersity in the matrix.[45-46] Interestingly, we observed that the incorporation of GO in the matrix substantially solubilize GOD, resulting in the formation of uniform BMF, as displayed in Figure 1 B. In the absence of GO, the SEM image of the BMF without GO displays micelle-like islands (Figure 1 A). Although the bonding of amphiphilic PMS to enzymes brings an increase in the global hydrophobic character of enzymes,[43-44] the strongly hydrophobic character of PS film yet makes it difficult to homogeneously disperse hydrophilic enzyme into hydrophobic PS film, leading to the formation of the micelle-like islands aggregated in BMF. On contrast, the presence of GO enables the relatively homogenous dispersion of GOD in the BMF (Figure 1 B), which could presumably be attributed to the electrostatic and/or hydrophobic interaction between GO and GOD.

Moreover, the incorporation of GO was found to stabilize the electron transfer mediator (i.e., Fc) in the BMF. Although Fc, ferrocenecarboxylic acid (Fc-COOH) and potassium

ferricyanide ($Fe(CN)_6^{3-}$) have been normally used as the mediators to shuttle the electron transfer between oxidases and electrode,[30] we selected Fc as the mediator because the positive charge feature of its oxidized form (i.e.. ferrocinium ion, Fc^+) enables its electrostatic interaction with the negatively charged GO, essentially providing a solution to stabilizing Fc in the BMF. Figure 2 compares the consecutive cyclic voltammograms (CVs) obtained at the GO-free BMF-based (A) and BMF-based (B) GC electrodes in aCSF solution. The voltammograms obtained with both electrodes display one pair of the redox wave, which was ascribed the redox process of Fc in the as-formed BMF. The striking difference between the voltammograms obtained with both electrodes lies in the stability of the electrodes with consecutive potential cycling; at the GO-free BMF-based electrode, both anodic and cathodic peak currents decrease gradually with consecutive potential cycling (A), demonstrating the leakage of Fc from the film. On contrast, at the BMF-based electrode, both anodic and cathodic peak currents remain almost unchanged with consecutive potential cycling (Figure 2 B), suggesting Fc was stably confined in the film. The GO-enhanced stability of the BMF was considered to mainly stem from the electrostatic interaction between Fc^+ and the negatively charged GO. To verify this hypothesis, we conducted control experiments by incorporating negatively charged electron transfer mediators such as Fc-COOH and $Fe(CN)_6^{3-}$ into the matrix to form BMF. Although both Fc-COOH and $Fe(CN)_6^{3-}$ were also easily incorporated into the PMS/PS matrix to form BMFs, the electrodes based on either kind of BMFs were not stable, which could be seen from the gradual decrease in both anodic and cathodic currents recorded with both electrodes with consecutive potential cycling (data not shown).

In addition, the incorporation of GO in the BMF actually endows the as-formed BMF with a good electrochemical property, as demonstrated in Figure 3. In aCSF, the BMF-based GC electrode exhibits one pair of well-defined redox wave, which was ascribed to the

electron transfer process of Fc incorporated in the BMF. Both cathodic and anodic peak potentials remain almost unchanged with increasing the potential scan rate employed (Figure 3A). In addition, the anodic (I_{pa}) and cathodic (I_{pc}) peak currents increase linearly with the potential scan rate (ν) (I_{pa} (nA) = 1.267 ν (mV s^{-1}) + 172.2, γ = 0.996; I_{pc} (nA)= -0.984 ν (mV s^{-1}) - 120.4 , γ = 0.996), suggesting that the redox process of Fc is a fast surface adsorption-dominating process. These features presumably demonstrate that the incorporation of GO into the BMF eventually maintain the fast electron transfer property of Fc mediator within the matrix, in addition to its role to stabilize Fc mediator in the BMF described above. The fast electron transfer property of the as-formed BMF could be a consequence for the efficient electrocatalysis of the BMF-based electrodes toward glucose, as depicted in (Figure 3 B). The CV of the BMF-based GC electrode in aCSF exhibits one pair of redox couple at a formal potential of +0.22 V, corresponding to one-electron redox process of the incorporated Fc (Figure 3 B, black curve), as mentioned above. The addition of 20 mM glucose leads to a significant increase in the oxidation current and a decrease in the reduction current of the redox couple of Fc mediator (Figure 3 B, red curve), demonstrating a good bioelectrochemical catalytic activity of the as-formed BMF toward glucose oxidation, which forms a straightforward basis for in vivo monitoring of glucose, *vide infra*.

In addition to the striking properties of the BMF formed with GO, GOD and Fc in PMS/PS matrix, the incorporation of GO into the matrix actually enables the as-formed BMF three-dimensionally conductive, which could be concluded from the in vitro experiments with the OECS with the GO-free BMF-based and BMF-based electrodes as the detector in the thin-layer electrochemical flow cell (Scheme 1 B). The comparison of the current responses of both systems toward the same concentration of glucose reveals that the incorporation of GO into the BMF substantially increases (almost by 6-fold) the sensitivity

of the as-prepared BMF-based biosensor, as displayed in Figure 4. The increase may be due to the formation of three-dimensional conducting structure of the BMF with the assistance of GO; GO actually acts as electron conductor in the film and thereby facilitate the electron transfer within the film.

Analytical Properties of BMF-based OECS. In order to evaluate the validity of the BMF-based biosensors for continuously monitoring the dynamic changes of glucose, the analytical properties of the BMF-based OECS including sensitivity, stability, reproducibility and selectivity were systematically investigated in vitro. Figure 5 A depicts the typical amperometric responses obtained with the BMF-based OCES toward glucose with aCSF as the perfusion solution. The system was well responsive toward the successive addition of glucose when the BMF-based biosensor was polarized at a constant potential of +0.20 V (*vs*. Ag/AgCl). The current was linear with the concentration of glucose within the concentration range from 50 to 500 μM (I (nA) = 0.30C_{glucose} (μM) + 29.5, γ = 0.9972) with a detection limit of 10 μM (S/N = 3). The stability and reproducibility of the BMF-based OECS were evaluated with 200 μM glucose standard solution. As shown in Figure 5 B and C, the OECS developed in this study was relatively stable and reproducible for the continuous monitoring of glucose; the current response toward 200 μM glucose remained unchanged after continuously running the measurements for more than 1 h (Figure 5 B). With aCSF as the perfusion solution and at a rate of 3 μL min^{-1}, the relative standard deviation of seven repeated glucose monitoring was 3.4% (C). All these results demonstrate the OECS with the BMF-based OECS possesses excellent analytical properties and could be used for reliable and durable in vivo monitoring of glucose in rat brain. We have also investigated the selectivity of the BMF-based OECS by perfusing the electroactive species endogenously coexisting in the brain microdialysate including E, NE, UA, AA, DOPAC and DA into the system. As could be seen in Figure 5 D, when the biosensor was poised at +0.20 V, the

perfusion of the species mentioned above at the concentrations higher than their physiological levels did not lead to obvious current responses, as compared with that of glucose, suggesting the system was virtually free from the interference from these species. These results well validate the OECS demonstrated in this study with the BMF-based biosensors as the detector for continuous measurements of microdialysate glucose in auditory cortex of rat brain.

Towards Continuous Monitoring of Microdialysate Glucose. In order to further validate the BMF-based OCES demonstrated here (Scheme 1 B) for in vivo measurement of glucose in the microdialysate collected from rat auditory cortex, we have conducted two experiments to study the in vivo stability of the BMF-based OECS and the change of the microdialysate glucose evoked by the local injection of insulin (5 U) to the animals continuously monitored with the OECS. Figure 6 shows the typical amperometric responses recorded with the BMF-based OECS toward the microdialysate continuously sampled from rat auditory cortex before and after local injection of insulin. As shown, BMF-based OECS was quite stable for continuously monitoring microdialysate glucose (A) and the *i.p.* injection of insulin clearly results in a large decrease of the response current toward microdialysate glucose (B), demonstrating that the biosensors developed with the rationally designed and constructed BMF could be used for in vivo monitoring glucose in the central nervous system by coupling with in vivo microdialysis because the administration of insulin has been demonstrated to reliably cause the decrease of glucose level.[47]

On the basis of the good properties of the BMF-based OECS investigated above, we applied the OECS for in vivo monitoring the dynamic change of the glucose level in rat auditory cortex during salicylate-induced tinnitus. Figure 7 depicts the typical amperometric responses recorded with the BMF-based OECS toward brain microdialysate continuously sampled from rat auditory cortex before and during transient tinnitus induced by sodium

salicylate. The basal level of microdialysate glucose collected from rat auditory cortex was determined to be 120 ± 10 μM (n = 5). After the rats were administrated with salicylate to induce transient tinnitus, the microdialysate glucose concentration in the rat auditory cortex remarkably increased to 433 ± 190 μM (n = 5) at the time point of 1.5 h, suggesting that the salicylate-induced tinnitus in rats occurs with a significant change of glucose metabolic activity in the central nervous system. As far as we know, the increase observed in this study at a level of living animals has not been reported before. Although the insight into the change of glucose following salicylate-induced tinnitus still necessitates more physiological studies, this observation is believed to be useful for understanding the molecular basis underlying the neurophysiological mechanisms of salicylate-induced tinnitus. These results substantially demonstrate that the BMF rationally designed and simply constructed in this study could be useful for in vivo monitoring of glucose and possibly other kinds of physiologically important species (by replacing GOD with other kinds of oxidases in the matrix) in the central nervous system.

CONCLUSIONS

In summary, we have demonstrated a new strategy for technically simple and reproducible preparation of in vivo electrochemical biosensors through rational designing and one-step formation of BMF that efficiently integrates oxidase, electron transfer mediator Fc, GO into PMS and PS matrix. The BMF-based biosensors exhibit efficient electrocatalysis toward the target with striking analytical properties including a high reliability and robustness. By directly coupling an electrochemical flow cell with the one-step constructed BMF-based biosensor as the detector to in vivo microdialysis, we have successfully established an OECS for online monitoring of glucose in the microdialysate continuously sampled from the auditory cortex of rat brain during salicylate-induced tinnitus

model. The BMF strategy demonstrated here essentially offers a technically simple and relatively versatile approach to in vivo measurements of neurochemicals in the brain of living animals, which is envisaged to be of great importance in understanding the molecular basis underlying brain functions.

ACKNOWLEDGMENTS

This research was financially supported by the NSF of China (21321003, 21210007, and 21435007 for LM, 21205008 for XW, 21275024 for SW), the Chinese Academy of Sciences, the Fundamental Research Funds for the Central Universities (DUT12LK31), and the Key Laboratory of Ocean Energy Utilization and Energy Conservation of Ministry of Education. We are deeply appreciated to Prof. Uchiyama Shunichi of Saitama Institute of Technology (Japan) for providing PMS.

REFERENCES

(1) Andrews, A. M.; Schepartz, A.; Sweedler, J. V.; Weiss, P. S. *J. Am. Chem. Soc*. **2014**, *136*, 1-2.

(2) Russell A. Poldrack. R. A.; Farah. M. J. *Nature* **2015**, *526*, 371-379.

(3) Trouillon, R.; Passarelli, M. K.; Wang, J.; Kurczy, M. E.; Ewing, A. G. *Anal. Chem*. **2013**, *85*, 522-542.

(4) Wilson, G. S.; Michael, A. C. Compendium of In Vivo Monitoring in Real-Time Molecular Neuroscience：Volume 1: Fundamentals and Applications, World Scientific Publications, **2014**.

(5) Silberberg，D.; Anand, N. P.; Michels, K.; Kalaria, R. N. *Nature* **2015**, *527*, 151-154

(6) Wilson, G. S.; Hu. Y. *Chem. Rev.* **2000**, *100*, 2693-2704.

(7) Robinson, D. L.; Hermans, A.; Seipel, A. T.; Wightman, R. M. *Chem. Rev.* **2008**, *108*, 2554-2584.

(8) Libby, P.; Ridker, P. M.; Hansson, G. K. *Nature* **2011**, *473*, 317-325.

(9) Wilson, G. S.; Johnson, M. A. *Chem. Rev.* **2008**, *108*, 2462-2481.

(10) Li, X.; Majdi, S.; Dunevall, J.; Fathali, H.; Ewing, A. G. *Angew. Chem. Int. Ed*. **2015**, *54*, 11978-11982.

(11) Wightman, R. M.; Storpe, E.; Plotsky, P. M.; Adams, R. N. *Nature* **1976**, *262*, 145-146.

(12) Paul, D. W.; Stenken, J. A.; *Analyst*, **2015**,*140*, 3709-3730.

(13) Zhou, Y.; Wong, J. T.; Mabrouk, O. S.; Kennedy, R. T. *Anal. Chem*. **2015**, *87*, 9802-9809.

(14) Michael, A. C.; Borland, L. M. *Electrochemical Methods for Neuroscience,* CRC Press, **2006**.

(15) Rogers, L. M.; Feuerstein, D.; Leong, C. L.; Takagaki, M.; Niu, X.; Graf, R.; Boutelle, M. G. *ACS Chem. Neurosci.* **2013**, *4*, 799-807.

(16) Zhang, M.; Liu, K.; Gong, K.; Su, L.; Chen, Y.; Mao, L. *Anal. Chem.* **2005**, *77*, 6234-6242.

(17) Iwasaki, Y.; Horiuchi, T.; Niwa, O. *Anal. Chem.* **2001**, *73*, 1595-1598.

(18) Yue, X.; Zhu, Z.; Zhang, M.; Ye Z. *Anal. Chem.* **2015**, *87*, 1839-1845.

(19) Hopwood, M. P.; Strong, A. J.; Boutelle, M. G. *Trends in Analytical Chemistry.* **2003**, *22*, 487-497.

(20) Hayashi, K.; Kurita, R.; Horiuchi, T.; Niwa, O. *Biosensors and Bioelectronics.* **2003**, *18*, 1249-1255.

(21) Ravenna, Y.; Xia, L.; Gun, J.; Mikhaylov, A. A.; Medvedev, A. G.; Lev, O.; Alfonta, L. *Anal. Chem*. **2015**, *87*, 9567-9571.

(22) Zhou, C.; Shi, Y.; Ding, X.; Li, M.; Luo, J.; Lu, Z.; Xiao, D. *Anal. Chem.* **2013**, *85*, 1171-1176.

(23) Leger, C.; Bertrand, P. *Chem. Rev.* **2008**, *108*, 2379-2438.

(24) Turner, A. P. F. *Chem. Soc. Rev*. **2013**, 42, 3184-3196.

(25) Wang, J. *Chem. Rev.* **2008**, *108*, 814-825.

(26) Song, Y.; Liu, H.; Tan, H.; Xu, F.; Jia, J.; Zhang, L.; Li, Z.; Wang, L. *Anal. Chem.* **2014**, *86*, 1980-1987.

(27) Zhou, Z.; Hartmann, M. *Chem. Soc. Rev*. **2013**, 42, 3894-3912.

(28) Yu, P.; Yan, J.; Su, L.; Zhang, J.; Mao, L. *J. Phys. Chem*. C **2008**, *112,* 2177-2182.

(29) Yu, P.; Zhou, H.; Cheng, H.; Qian, Q. Mao, L. *Anal. Chem*. **2011**, *83*, 5715-5720.

(30) Zhuang, X.; Wang, D.; Lin, Y.; Yang, L.; Yu, P.; Wei, J.; Mao, L. *Anal.Chem*. **2012**, *84*, 1900-1906.

(31) Huang, P.; Mao, J.; Yang, L.; Yu, P.; Mao, L. *Chem. Eur. J.* **2011**, 17, 11390-11393.

(32) Lu, X.; Cheng, H.; Huang, P., Yang, L.; Yu, P.; Mao, L. *Anal. Chem.* **2013**, *85*, 4007-4013.

(33) Zhang, M.; Yu, P.; Mao, L., *Acc. Chem. Res.* **2012**, *45*, 533-543.

(34) Lin, Y.; Yu, P.; Hao, J.; Wang, Y.; Ohsaka, T.; Mao, L. *Anal. Chem*. **2014**, *86*, 3895-3901.

(35) Hagiwara, T.; Suzuki, I.; Takeuchi, K.; Hamana, H.; Narita, T. *Macromol.* **1991**, *24*, 6856-6858.

(36) Wang, X.; Wang, J.; Cheng, H.; Yu, P.; Ye, J.; Mao. L. *Langmuir* **2011**, *27*, 11180-11186.

(37) Hummers, W. S., Offeman, R. E. *J. Am. Chem. Soc*. **1958**, *80*, 1339-1339.

(38) Liu, K.; Lin, Y.; Xiang, L.; Yu, P.; Su, L.; Mao, L. *Neurochemistry International* **2008**, *52*, 1247-1255.

(39) Liu, K.; Lin, Y.; Yu, P.; Su, L.; Mao, L. *Brain Research* **2009, *1253*,** 161-168.

(40) Paxinos, G., Watson, C. *The Rat Brain in Stereotaxic 542 Coordinates;* Academic Press: San Diego, **1997**.

(41) Jung, T. T.; Hwang, A. L.; Miller, S. K.; Rhee, C. K.; Park, Y. S. *Acta Oto-laryngolgica.* **1995**, 115, 251-254.

(42) Yang, G.; Lobarinas, E.; Zhang, L.; Turner, J.; Stolzberg, D.; Salvi R.; Sun, W. *Hear. Res*. **2007**, *226*, 244-253.

(43) Wang, X.; Watanabe, H.; Uchiyama, S. *Talanta* **2008**, *74*, 1681-1685.

(44) Wang, X.; Hagiwara, T.; Uchiyama, S. *Anal. Chim. Acta* **2007**, *587*, 41-46.

(45) Chen, D.; Feng, H.; Li, J. *Chem. Rev.* **2012**, *112*, 6027-6053.

(46) Georgakilas, V.; Otyepka, M.; Bourlinos, A. B.; Chandra, V.; Kim, N.; Kemp, K. C.; Hobza, P.; Zboril, R.; Kim, K. S. *Chem. Rev.* **2012**, *112*, 6156-6214.

(47) Canfora, E. E.; Jocken, J. W.; Blaak, E. E. *Nature Reviews Endocrinology* **2015,** *11*, 577-591.

Scheme 1 - L. Mao *et al.*

Scheme 1. Schematic Illustration of BMF Preparation (A) and OECS with BMF-based Biosensor as Detector (B).

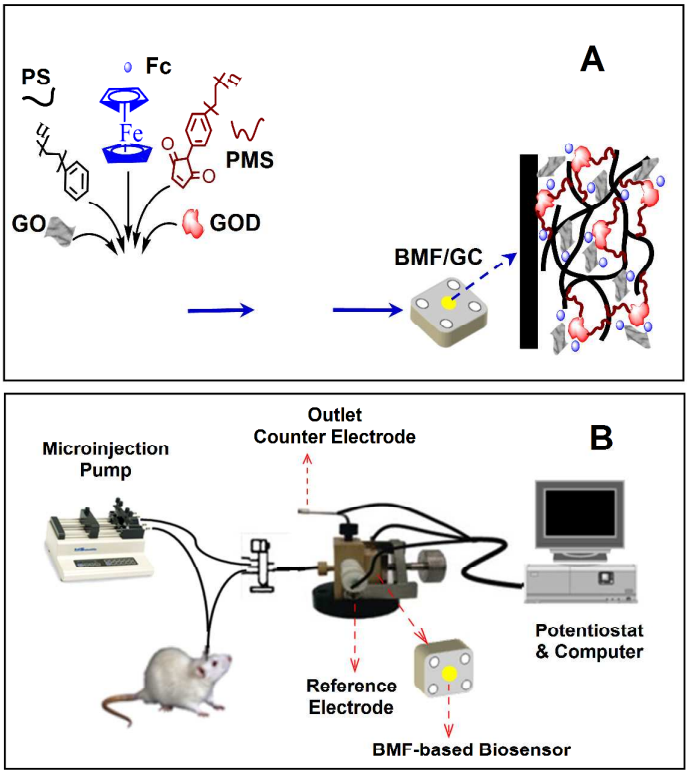

The BMF was prepared by mixing solutions of GOD, GO, Fc, PMS and PS to form homogenous dispersion and then drop-coating the dispersion onto glassy carbon (GC) substrate. The OECS was established by directly coupling an electrochemical flow cell with BMF-based biosensor as the detector to in vivo microdialysis for online monitoring glucose in the microdialysate continuously sampled from auditory cortex of rat brain during salicylate-induced tinnitus.

Figure 1 - L. Mao *et al.*

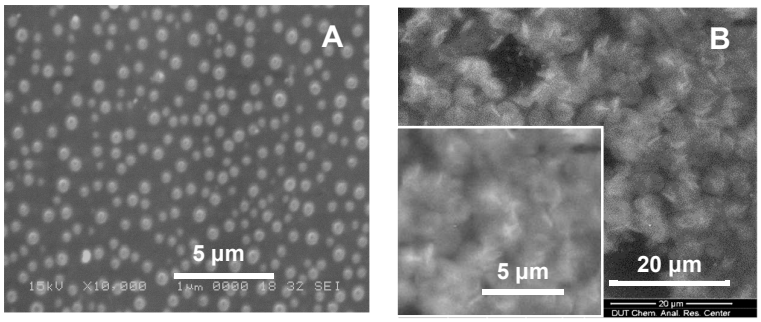

Figure 1. SEM images of the films of GOD/PMS/PS (A) and GO/Fc/GOD/PMS/PS (B) coated on GE electrodes.

Figure 2 - L. Mao *et al.*

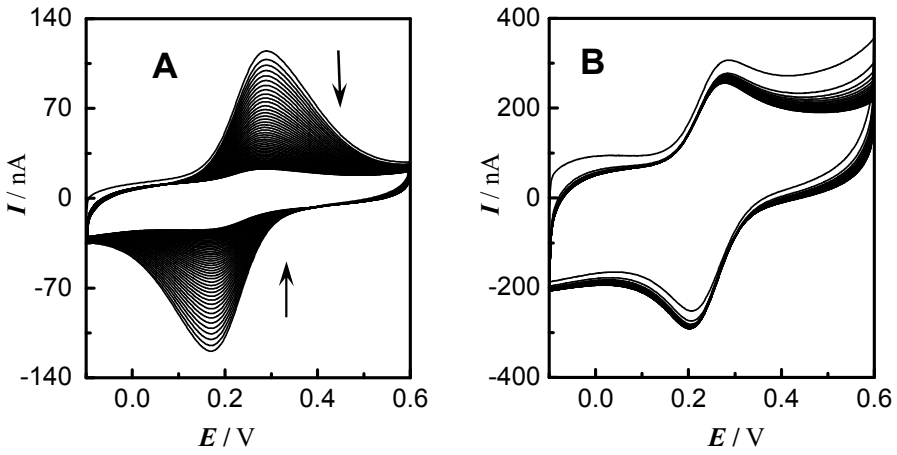

Figure 2. Typical consecutive CVs for 50 segments obtained at the GO-free BMF-based (A) and BMF-based (B) GC electrodes in aCSF (pH 7.20). Scan rate, 50 mV s^{-1}.

Figure 3 - L. Mao *et al.*

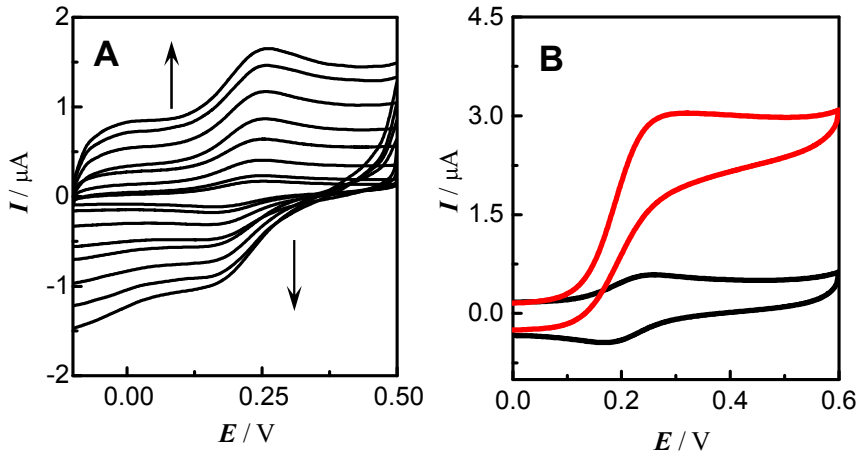

Figure 3. A) CVs at the BMF-based GC electrode in aCSF (pH 7.20) at different scan rates of 10, 20, 50, 100, 200, 300, 400 and 500 mV s^{-1} (from inner to outer). B) Typical CVs obtained at the BMF-based GC electrode in aCSF (pH 7.20) before (black curve) and after (red curve) the addition of 20 mM glucose. Scan rate, 40 mV s^{-1}.

Figure 4 - L. Mao *et al.*

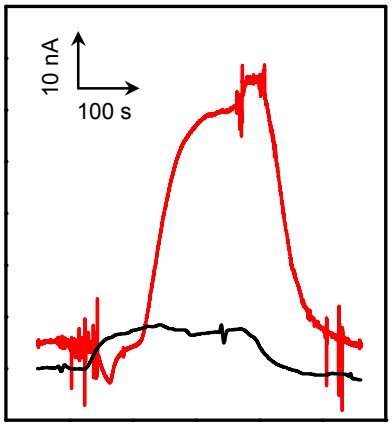

Figure 4. Online amperometric responses of OECS with GO-free BMF-based (black curve) and BMF-based (red curve) electrodes as the detectors toward 100 μM glucose. The electrodes were polarized at +0.20 V. Flow rate was 3 μL min^{-1}.

Figure 5 - L. Mao *et al.*

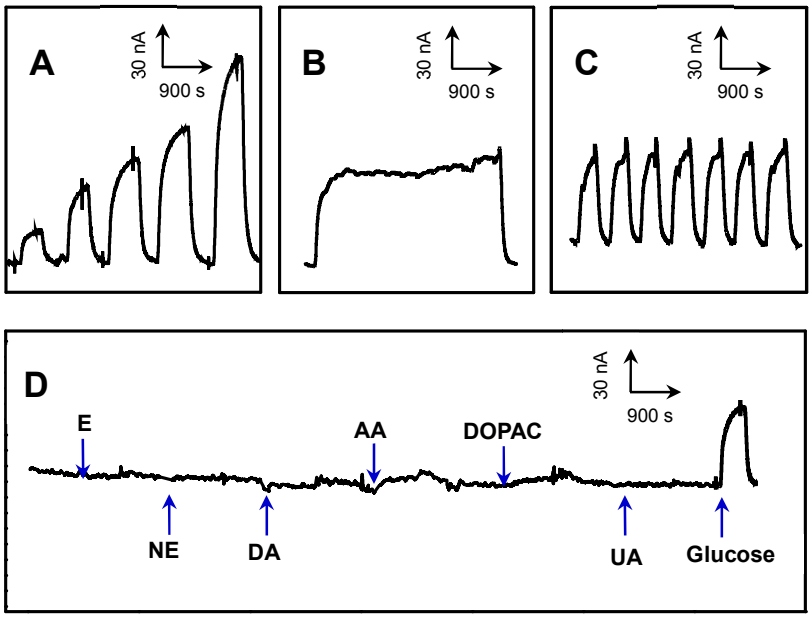

Figure 5. A) Typical amperometric responses obtained with the OECS with BMF-based biosensor as the detector toward successive addition of glucose with different concentrations of 50, 100, 200, 300 and 500 μM. B) and C) Representative amperometric response repeatedly (B) and continuously (C) recorded with the BMF-based OECS toward 200 μM glucose standards. D) Typical amperometric responses obtained with the BMF-based OECS toward E, NE, DA, DOPAC, UA (10 μM of each species), AA (5 μM) and glucose (100 μM) in aCSF (pH 7.20). The arrows indicate the perfusion of the solutions of each kind of the species studied. Other conditions were the same as those in Figure 4.

Figure 6 - L. Mao *et al.*

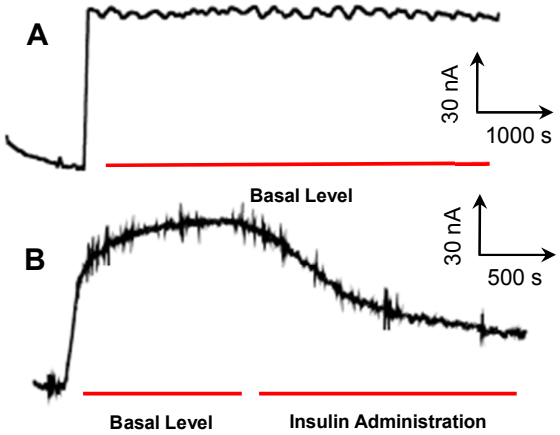

Figure 6. Typical amperometric responses recorded with the BMF-based OECS toward brain microdialysate continuously sampled from rat auditory cortex before (A) and after (B) administration of insulin (5 U). The electrode was polarized at +0.20 V. Flow rate, 2 µL min^{-1}.

Figure 7 - L. Mao *et al.*

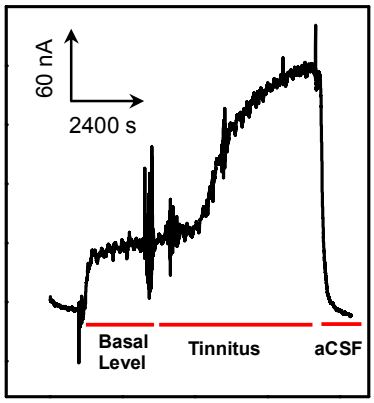

Figure 7. Typical amperometric responses recorded with the BMF-based OECS toward brain microdialysate continuously sampled from rat auditory cortex before and during transient tinnitus induced by sodium salicylate. Other conditions were the same as those in Figure 6.

For TOC only